

Tube-wave suppression in single-well seismic acquisition

Thomas M. Daley, Roland Gritto and Ernest L. Majer

*Center for Computational Seismology, Lawrence Berkeley National Laboratory
Berkeley, CA*

Phillip West

Idaho National Engineering and Environmental Laboratory

(March 21, 2002)

ABSTRACT

Single well seismic imaging is significantly hampered by the presence of borehole tube-waves. A tube-wave suppressor has been tested using single-well seismic equipment at the Lost Hills (California) oil field. The suppressor uses a gas filled bladder kept slightly above borehole fluid pressure. The field tests show a measurable reduction in tube-wave energy as compared to body waves propagating in the surrounding reservoir rock. When using a high-frequency (500 - 4000 Hz) piezoelectric source, the P-wave to tube-wave amplitude ratio is increased by 33 dB. When using a lower frequency (50 - 350 Hz) orbital vibrator source, the S-wave to tube-wave amplitude ratio was increased by 21 dB while the P-wave to tube-wave amplitude ratio was increased by 23 dB. These reductions in tube-wave amplitudes significantly improve single-well data quality.

INTRODUCTION

Single-well seismic data provide a scale of investigation which is intermediate between sonic log data and crosswell seismic data. In single-well seismic acquisition a seismic source and seismic sensors with designs appropriate for crosswell surveys are placed in the same borehole. In recent years, single-well seismic has been investigated as a means to extend the resolution of well logging, as well as provide imaging capability in areas not easily accessible with conventional crosswell or vertical seismic profiles (VSP), e.g. salt flank imaging. An inherent and significant problem for single-well seismic surveys is borehole tube-waves, as shown in numerical models (Kurkjian, et al., 1994; Coates, 1998). One of the detrimental effects modeled and observed is the masking of body-wave reflections by the tube-wave. Single-well seismic field experiments have been conducted by Lawrence Berkeley National Laboratory (LBNL) to develop and improve single-well seismic methodology (Majer, et al., 1997; Daley, et al, 2000a), however the tube-wave remains a significant problem. The results in this paper demonstrate the successful implementation of a tube-wave suppressor in a single-well survey.

Tube-waves propagate in a fluid filled borehole with amplitudes often much larger than body-waves in the surrounding rock. A tube-wave is an interface wave for a cylindrical interface between two media, typically a borehole fluid and surrounding elastic rock. Borehole waves were described by Lamb (1898), and were observed in the early twentieth century (Sharpe, 1942; Ording and Redding, 1953) as summarized by White (1965). Using trapped (or guided) mode analysis, the classic tube-wave can be seen as the lowest order trapped mode (Schoenberg, et al., 1981). Higher order modes may be generated depending on material properties and source frequency. While the fundamental mode is usually called a Stoneley wave, the term Scholte wave is perhaps more appropriate for a solid-liquid interface.

Throughout many years of borehole seismology development, tube-waves have

most often been considered a problematic source of "noise" to those trying to measure material properties in the medium surrounding the borehole. Some work has been done to analyze tube-wave attributes to estimate rock properties (for example, (Cheng, et al, 1987; Kostek, et al, 1998). This analysis, when successful, is limited to near-borehole information because tube-waves decay quickly with increasing distance from the fluid-rock interface. While single-well data does present an opportunity for large scale tube-wave logging, our work is focused on imaging features away from the borehole and, therefore, the tube-wave is noise. We present here a description of the tube-wave suppressor designed at Idaho National Engineering and Environmental Laboratory (INEEL) followed by a description of field tests at the Lost Hills, California oil field and an analysis of the field tests which quantifies the reduction in tube-wave to body-wave amplitude ratio. Note that English units will be used because they were used in the suppressor design and the field experiment acquisition.

TUBE-WAVE SUPPRESSOR DESIGN

Since the late 1990's INEEL has been working with LBNL to develop and deploy a tube-wave suppressor (TWS) specifically for use in singlewell seismic surveys (West, et al., 2002). The design deployed in this test uses a polymer bladder inflated to a pressure slightly higher than ambient borehole pressure.

The INEEL TWS is comprised of three major components (shown schematically in Figure 1) as follows: 1) pressure chamber with lower excess flow valve, 2) wire feed though, 3) bladder chamber containing the bladder and pressure control system. The pressure chamber is approximately 6 ft (1.8 m) long in a 10 ft (3 m) outer shell and is fabricated from 3 inch (0.08 m) stainless steel pipe. It has been designed and tested per the requirements of ASME section VIII and B31.3 for a pressure rating of 2000 psi ($1.7 \cdot 10^7$ Pa). The chamber includes on its top, a safety relief valve, an outlet port (to a regulator), and on its bottom, an input fill valve and an excess flow valve. The excess

flow valve is configured to retain gas pressure internally to the chamber but opens when pressure differential to the borehole is minimal allowing equalization to borehole pressure by intaking borehole fluid. The wire feed through is comprised of a heavy wall 1" (0.025 m) diameter tube with O-ring surfaces on each end. The feed through accepts connectors configured for multiple sensors (currently 56 wire maximum for 22 gauge wire). The pressure regulation system, contained within the bladder chamber, is a fail-open, dual-stage assembly with excess pressure dump valves. The system is based on a scuba diving regulator system but re-configured for extended depth. The second stage is extremely sensitive and can provide gas flow control over a range of a few inches of water pressure. The assembled system also includes ascent pressure control valving (to dump excess pressure to the borehole). The bladder is a soft polymer cylinder, attached to the regulator outlet. The bladder and the regulator are contained within a perforated steel chamber for protection.

For field operation, the chamber is pressurized using gas (nitrogen) prior to deployment. Once in the borehole fluid, the regulator maintains the volume of the bladder with nitrogen at pressure slightly more than ambient. We believe the bladder provides pressure wave attenuation and energy dissipation. This implies that the bladder, which is exposed to the borehole fluid through perforations in the surrounding steel chamber, transfers tube-wave energy into heat as the compressional component of the tube-wave excites oscillations of the gas in the bladder. When deployed to depths where borehole pressure exceeds the storage chamber's internal pressure, the excess flow valve opens allowing the storage chamber's gas to be compressed by the borehole fluid and thereby maintaining bladder pressure. This borehole fluid pressurization allows operation at greater depths than the 2000 psi ($1.4 \cdot 10^7$) maximum initial pressure.

Figure 1 shows a photo of the INEEL TWS. The first deployment of the current design as part of LBNL's single-well system was in 1998 at a Baker-Atlas test well in Houston, however, the result was inconclusive (Daley, et al, 2000a). In early 2001, the

TWS was field tested with positive results in shallow (100 m) wells at the University of California's Richmond Field Station (RFS) (Daley and Gritto, 2001). In those tests, tube-wave attenuation of 9 to 11 dB was measured with respect to body-wave amplitudes. Following the success of the RFS tests, further tests were conducted to measure the effectiveness in deeper wells with higher fluid pressures and faster rock velocities. These tests were conducted at Chevron's Lost Hills oil field in California, as part of LBNL's singlewell and crosswell seismic field experiments at a CO₂ injection site.

FIELD TESTS

The Lost Hills site is a producing oil field undergoing enhanced oil recovery as a pilot CO₂ injection project. Figure 2 shows the location of the Lost Hills field. Observation wells were specifically drilled to allow geophysical monitoring of the CO₂ injection. Well OB-C1 was used as part of combined crosswell and singlewell seismic surveys (Daley, et al, 2000b) as well as the TWS testing described here. The well was cased with 7" (0.18 m) fiberglass casing, with an inside diameter (ID) of 6" (0.15 m), which was hung from 9 5/8" (0.24 m) steel surface casing at about 1000 ft (300 m) depth. The well was water filled with small amounts of leaked hydrocarbons in the fluid. Table 1 has the material properties of the casing and borehole fluid, as well as P- and S-wave velocities obtained from single-well and crosswell data acquisition at the site.

For single well data acquisition, the TWS was placed in LBNL's single-well equipment string between the source and sensors, as shown in Figure 3. Two tests were analyzed; one with a high frequency piezoelectric source and one with a lower-frequency orbital vibrator source (Daley and Gritto, 2001). These tests will be discussed individually.

Piezoelectric Source Test

The initial test used LBNL's piezoelectric source and hydrophone receivers for a single well survey between 1300 and 2000 ft (396 - 610 m) at 2 ft (0.6 m) intervals. Unfortunately, after acquiring the single well survey with the TWS, the hydrophone cable failed and a companion survey without the TWS could not be obtained. However, in previous work at this site, LBNL had obtained a single well survey in the same well, covering the same depths, without the TWS. This previous work was part of a pre CO₂ injection baseline survey. The only significant change was that different hydrophone sensors were used so absolute amplitudes can not be compared. However, absolute amplitudes are not necessary since our analysis uses amplitude ratios between body waves and tube-waves. The same source and recording system were used in both surveys. Because the new sensor string had a longer lead-in cable and different sensor spacing, we limit our analysis to a sensor with the same source-receiver separation (offset). Using these data, the preinjection and postinjection single-well surveys form a data set to compare the piezoelectric-source, hydrophone-sensor data recorded with and without TWS.

Figure 4 shows the seismograms for a single channel gather (equivalent to a common offset gather) for the two surveys. In the surveys with and without TWS the source-receiver offset was 90 ft and 89 ft (27.4 and 27.1 m), respectively. The qualitative reduction in tube-wave energy when using the TWS, as compared to P-wave energy, is clearly visible in the seismograms. In order to quantify the difference, we calculated the RMS amplitude of an 11 sample (1.375 ms) moving window averaged for 16 representative traces and plotted this result in dB (relative to the trace's maximum) as a function of time. This analysis, from the commercial processing package FOCUS-3D, calculates the RMS value $e(t)$ for a time window where $e(t) = \sqrt{[f(t)^2 + h(f(t))^2]}$ for recorded data $f(t)$, and where $h(f(t))$ is the Hilbert transform of the recorded data. Figure 5 shows this amplitude analysis for the data

with and without TWS. The wave types (P-wave and tube-wave) were identified using arrival time. The data recorded without TWS has tube-wave amplitude 12 dB more than the P-wave amplitude. The data recorded with the TWS has tube-wave amplitude 21 dB below the P-wave amplitude. The total increase in P-wave to tube-wave amplitude ratio is therefor 33 dB.

Orbital Vibrator Source Test

A pair of tests was performed with and without the TWS using LBNL's orbital vibrator (OV) seismic source. In these tests, the data acquisition was repeated at the same time (post CO₂ injection) with no change in equipment except for removing the TWS. The OV source generates circularly polarized waves which can be decomposed into two perpendicular, horizontal, linearly oscillating sources, i.e. x and y components of motion (Daley and Cox, 2001). Although this source has minimal volumetric change, and therefor should generate relatively low amplitude tube-waves, it has been reported to generate tube-waves with amplitudes 20 dB greater than P-waves (Ziolkowski, et al, 1999). In a single well acquisition geometry, the orbital vibrator is expected to generate S-waves as the largest vertically propagating body wave.

For the OV data acquisition we used a 5-level string of 3-component wall-locking geophones. Therefore, this data set has 6-components of motion, 2 source components (x and y) and 3 sensor components (z, x, and y). These 6-component data sets, with and without TWS, are shown in Figure 6 for one receiver gather (common offset of 86 and 88 ft (26.2 and 26.8 m)). A single geophone component of the data is shown in Figure 7. As with the piezoelectric source data, the OV data with TWS has a clear reduction in tube-wave energy as compared to the same survey without TWS. Gain analysis was performed on the two OV data sets, again using an 11 sample window (2.75 ms) averaged for 5 representative traces from the Y-component source and Y-

component sensor (shown in Figure 7). Figure 8 shows the results of this amplitude analysis for the OV data recorded with and without TWS. With the TWS, the shear-wave has amplitude 16 dB greater than the tube-wave; whereas without the TWS, the shear-wave is at least 5 dB lower amplitude than the tube-wave. The actual ratio may be greater because the highest amplitude in the shear-wave arrival time-window for the case without TWS appears to be tube-wave multiples (see Figure 7). This is an inherent problem because the tube-wave is faster than the shear-wave in the Lost Hills diatomite. Nonetheless, we can obtain a lower bound for the amplitude ratio. The improvement in shear-wave to tube-wave amplitude ratio is at least 21 dB. The P-wave is relatively weak in the OV data (as expected for sensors vertically below a horizontally polarized source), however a small peak is seen in the amplitude analysis of Figure 8 at the expected arrival time of a P-wave. The improvement in P-wave to tube-wave amplitude ratio associated with this peak is about 23 dB (+3 dB with TWS versus -20 dB without TWS).

CONCLUSIONS

The tube-wave suppressor designed and built by INEEL was successfully tested at oil-field scales with a single well seismic acquisition system. In tests with a piezoelectric source and hydrophone sensors, the P-wave to tube-wave amplitude ratio was increased by 33 dB. In tests with an orbital vibrator source and wall-locking geophone sensors, the S-wave to tube-wave amplitude ratio was increased by 21 dB, and the P-wave to tube-wave amplitude ratio was increased by 23 dB. These are significant reductions. In fact, the shear-wave generated by the orbital vibrator source was only visible when using the TWS. The TWS design should allow operation at depths greater than those tested here, and in principle, allow deployment of multiple tools.

We believe these results are sufficient to justify the use of this tool in future single well experiments. Furthermore, we expect that multiple tools, or multiple bladders

on one tool, would increase the tube-wave suppression. The results presented here demonstrate a method for improved seismic data quality in single-well experiments. It is likely that similar results can be obtained in crosswell, VSP or other borehole seismic experiments.

REFERENCES

- Balch, A.H. and Lee, M.W., editors, 1984, Vertical Seismic Profiling: Technique, Applications, and Case Histories, International Human Resources Development Corporation, Boston, MA
- Cheng, C. H. and Jinzhong, Z. and Burns, D. R., 1987, Effects of in-situ permeability on the propagation of Stoneley tube waves in a borehole, *Geophysics*, **52**, 1279-1289.
- Coates, R. T., 1998, A modelling study of open-hole single-well seismic imaging, *Geophy. Prosp.*, **46**, p153-175.
- Daley, T.M., Majer, E.L., Gritto, R., 2000a, Single well seismic imaging - Status Report, Lawrence Berkeley National Laboratory Report LBNL-45342, Berkeley, Ca.
- Daley, T.M., Majer, E.L., Gritto, R., and Benson, S.M., 2000b, Borehole Seismic Monitoring of CO₂ Injection in a Diatomite Reservoir, American Geophysical Union 2000 Fall Meeting, EOS, v81, n48, Nov. 28, 2000.
- Daley, T.M. and Gritto, R., 2001 Field Tests of INEEL Tube-wave Suppressor and LBNL Borehole Seismic System at Richmond Field Station, February 2001, Lawrence Berkeley National Laboratory Report LBNL-49015, Berkeley, CA.
- Daley, T.M. and Cox, D., 2001, Orbital vibrator seismic source for simultaneous P- and S-wave crosswell acquisition, *Geophysics*, **66**, 1471-1480.

- Kostek, S., Johnson, D. L. and Randall, C. J., 1998, The interaction of tube waves with borehole fractures, Part I: Numerical models, *Geophysics*, **63**, p800-808.
- Kurkjian, A. L., Coates, R. T., White, J. E. and Schmidt, H., 1994, Finite-difference and frequency-wavenumber modeling of seismic monopole sources and receivers in fluid-filled boreholes, *Geophysics*, **59**, p1053-1064.
- Lamb, H., 1898, On the velocity of sound in a tube, as affected by the elasticity of the walls, *Manchester Memoirs*, v42, pp 1-16.
- Majer, E.L., Peterson, J.E., Daley, T.M., Kaelin, B., Myer, L., Queen, J., Peter D'Onfro, and Rizer, W., Fracture detection using crosswell and single well surveys, *Geophysics*, **62**, p495-504.
- Ording, J.R., and Redding, V.L., 1953, Sound waves observed in mud-filled well after surface dynamite charges, *J. Acoust. Soc. Am.*, **25**, p 719-726.
- Schoenberg, M., Marzetta, T., Aron, J., Porter, R.P., Space-time dependence of acoustic waves in a borehole, *J. Acoust. Soc. Am.*, **70**, p1496-1507.
- Sharpe, J.A., 1942, The production of elastic waves by explosion pressures. II. Results of observations near an exploding charge, *Geophysics*, **7**, 311-321.
- West, P.B., Weinberg, D.M., and Fincke, J.R., Empirical study of tube wave suppression for single well seismic imaging, Idaho National Engineering and Environmental Laboratory Report, INEEL/EXT-02-00274, Idaho Falls, Idaho.
- White, J.E., 1965, *Seismic Waves: Radiation, Transmission, and Attenuation*, McGraw-Hill, Inc., 302p.
- Ziolkowski, A., Sneddon, Z. and Walter, L., 1999, Determination of tube-wave to body-wave ratio for Conoco borehole orbital source, 69th Ann. Internat. Mtg. Soc. of Expl. Geophys., 156-159.

ACKNOWLEDGMENTS

This work was supported by the Assistant Secretary for Fossil Energy, Office of Natural Gas and Petroleum Technology, the Natural Gas and Oil Technology Partnership program, of the U.S. Department of Energy under Contract No. DE-AC03-76SF00098. Data processing was performed at the Center for Computational Seismology which is supported by the Director, Office of Science, Office of Basic Energy Sciences, Division of Engineering and Geosciences, of the U.S. Department of Energy under Contract No. DE-AC03-76SF00098. Thanks to Cecil Hoffpauir and Don Lippert of LBNL for help with SWSI equipment development and data acquisition, and Mike Morea of Chevron for support at Lost Hills field, and to the members of the Single Well Seismic Imaging project (<http://www-esd.lbl.gov/CCS/swsi.html>).

APPENDIX A: TUBE WAVE PROPERTIES AND IDENTIFICATION

Tube-waves are typically identified by one or more of the following characteristics: large amplitude (relative to body waves), reverberant waveform, elliptical particle motion, and/or velocity (which is generally slower than body waves). In our field example we identify the tube-waves by their velocity, which is intermediate between the formation P- and S-velocity. To ensure the identification of the tube-wave, we will solve for the expected velocity at the field site used to acquire the data presented here. The following solution for the velocity of a tube-wave in cased and uncased wells in an infinite solid (assuming the wavelength is long compared to the borehole radius) was developed by White (1965). For an uncased well the tube-wave velocity, C_T , is

$$C_T = \left[\rho \left(\frac{1}{K} + \frac{1}{\mu} \right) \right]^{-\frac{1}{2}} \quad (1)$$

where ρ and K are the fluid density and bulk modulus, respectively, and μ is the rock shear modulus. This velocity can also be expressed in terms of P- and S-wave velocities, α and β respectively, as follows (Balch and Lee, 1984):

$$C_T = \left(\frac{1}{\alpha_1^2} + \frac{\rho_1}{\rho_2 \beta_2^2} \right)^{-\frac{1}{2}} \quad (2)$$

where subscript 1 is for the borehole fluid and subscript 2 is for the surrounding rock. For a cased well, White (1965) gives the tube-wave velocity as:

$$C_T = \left[\rho \left(\frac{1}{K} + \frac{1}{\mu + \left(\frac{Eh}{2b} \right)} \right) \right]^{-\frac{1}{2}} \quad (3)$$

where K is the borehole fluid bulk modulus, μ is the rock's shear modulus, E is the casing's Young's modulus, h is the casing wall thickness and b is the borehole radius. It is known, but remains notable, that the cased well tube-wave velocity is significantly faster than the open hole tube-wave velocity for the same borehole.

Our field tests were conducted in a fiberglass-cased observation well with water as the borehole fluid. Using equation 3 and the parameters in Table 1, the calculated

tube-wave velocity for the well is 987 m/s (3200 ft/s). The velocity of the seismic arrival we identify as a tube-wave in Figure 4 varies from 975 to 1035 m/s (3200 to 3400 ft/s). Thus, allowing for some variation in fluid and formation properties, the measured tube-wave velocities in our field test agree with the calculated velocity, thereby confirming our identification of the tube-wave.

TABLES

Table 1: Well OB-C1 Material Properties

Fluid P-wave Velocity (m/s)	1500
Fluid Density (kg/m^3)	1000
Rock Density (kg/m^3)	1600
Rock S-wave Velocity (m/s)	800
Rock P-wave Velocity (m/s)	1675
Casing Wall Thickness (m)	0.0125
Casing Radius (m)	0.09
Casing Young's Modulus (N/m^2)	1.0×10^{10}

FIGURES

FIG. 1. INEEL tube-wave suppressor in schematic (left) and as deployed at Lost Hills (right) as part of LBNL's single well seismic equipment.

FIG. 2. Oil fields of southern San Joaquin Valley, California. Lost Hills is northwest of Bakersfield, Ca.

FIG. 3. Schematic drawing of LBNL single-well seismic acquisition system with tube-wave suppressor.

FIG. 4. Common offset gathers of single-well seismic data recorded with (left) and without (right) a tube-wave suppressor. Both data sets were acquired with a piezoelectric source and hydrophone receivers. Each trace is normalized by its own maximum amplitude. The reduction in tube-wave energy with respect to P-wave energy is easily visible.

FIG. 5. Amplitude analysis of piezoelectric source singlewell data recorded with (left) and without (right) the TWS. The amplitudes are RMS in dB down from the maximum for a moving window averaged over 16 traces. The data without TWS has peak amplitude (0 dB) from source electrical crosstalk at zero time (not plotted). Comparison of the plots shows the TWS has increased the ratio of P-wave to Tube-wave RMS amplitude by 33 dB (21 dB + 12 dB).

FIG. 6. 6-component single well data acquired with the orbital vibrator source and 3-component wall-locking geophone sensors. These data are a common offset gather (offset = 86 ft with TWS on left and 88 ft without TWS on right). The top and bottom rows are the two sourcecomponents (X and Y) as measured by the three sensor components (Z, X, and Y). The data has been trace normalized (each trace

normalized to its own maximum). The horizontal component data outlined in red was selected for analysis and is shown in Figure 7.

FIG. 7. Orbital-vibrator source, single-well data in a common offset gather for a horizontal geophone with TWS (left) and without TWS (right). Data are shown at true relative amplitude. The reduction in tube-wave energy when using the TWS is sufficient to allow identification of a shear-wave arrival (left), which is not identifiable in the data without a TWS (right).

FIG. 8. RMS amplitude analysis of orbital vibrator single well data recorded with (left) and without (right) a TWS. For the data recorded without a TWS, the tube-wave is the largest arrival. In data recorded with the TWS, the S-wave is the largest amplitude arrival. Comparing the amplitudes at the S-wave arrival time, we observe a 21 dB improvement in S-wave to tube-wave amplitude ratio. The improvement in P-wave to tube-wave amplitude ratio is 23 dB.

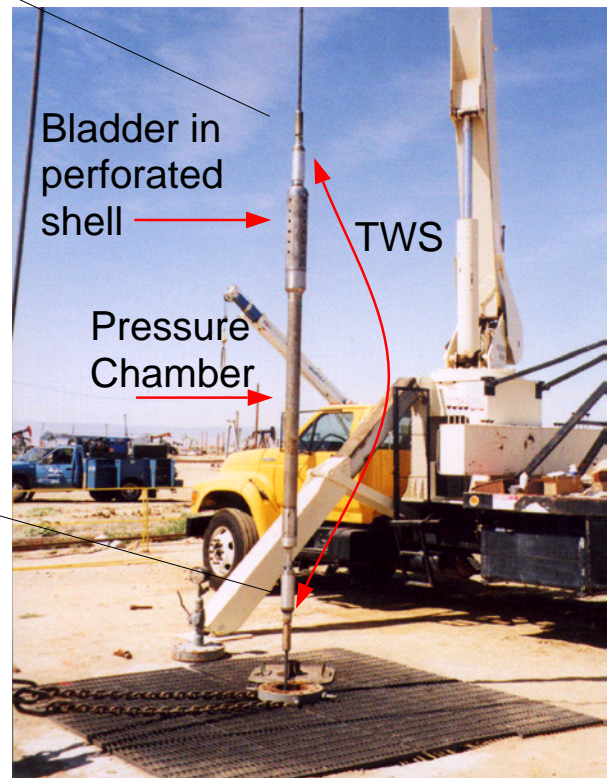
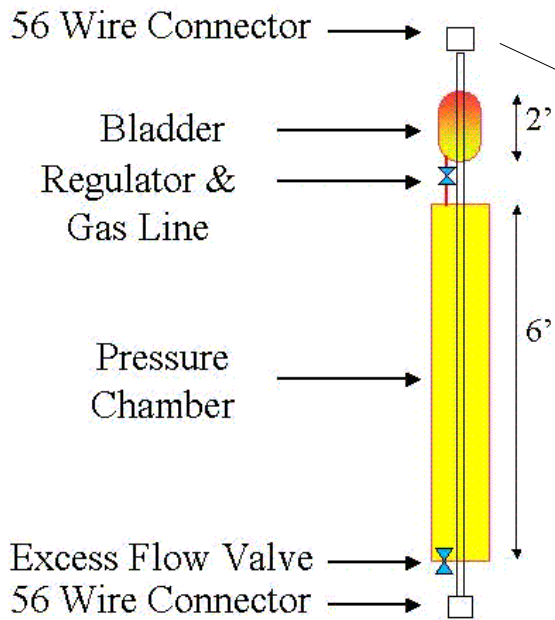


Figure 1. INEEL tube-wave suppressor in schematic (left) and as deployed at Lost Hills (right) as part of LBNL's single well seismic equipment.

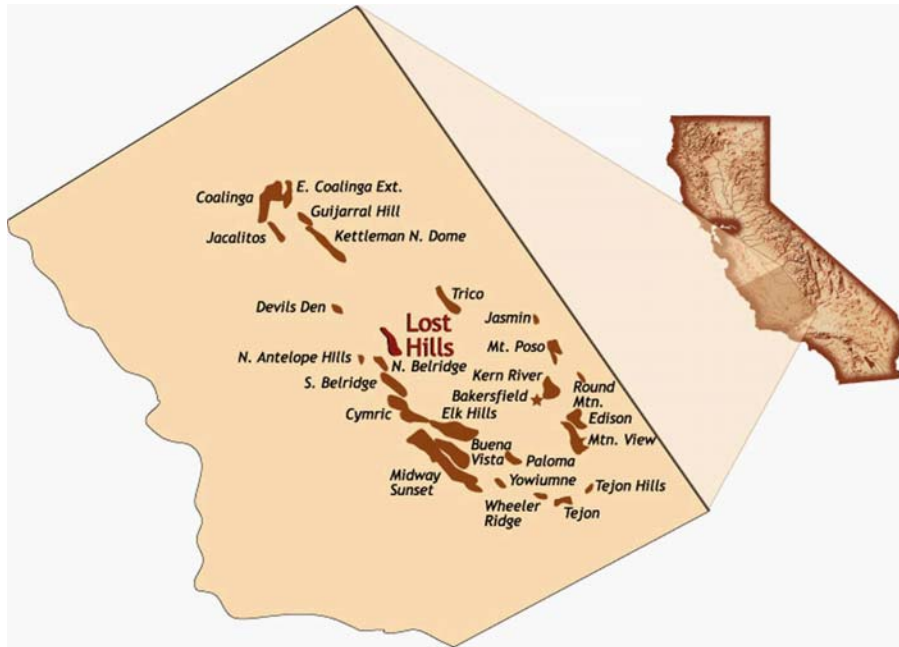


Figure 2. Oil fields of southern San Joaquin Valley, California. Lost Hills is north-west of the city of Bakersfield, Ca.

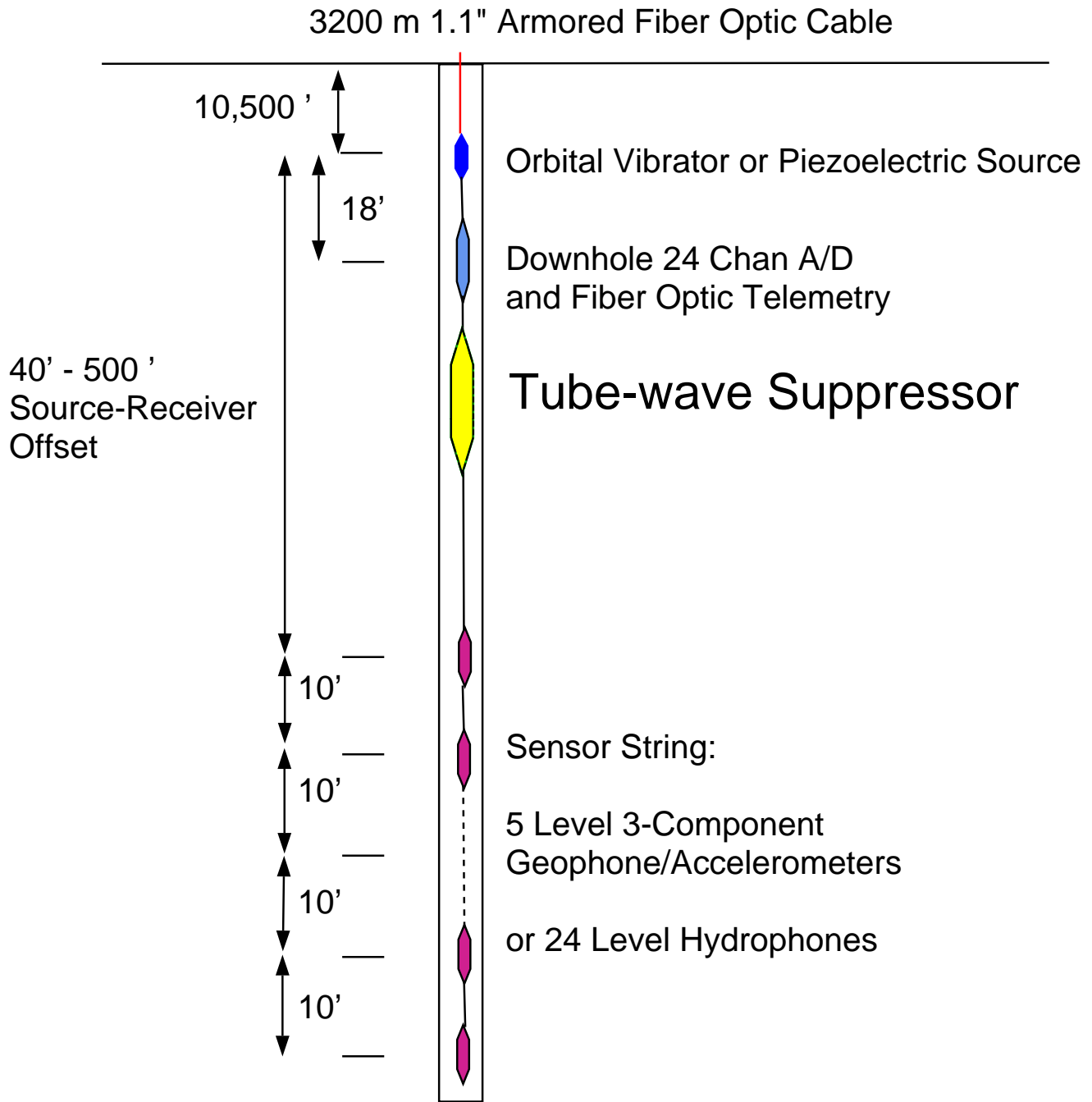


Figure 3 Schematic drawing of LBNL single-well seismic acquisition system with tube-wave suppressor.

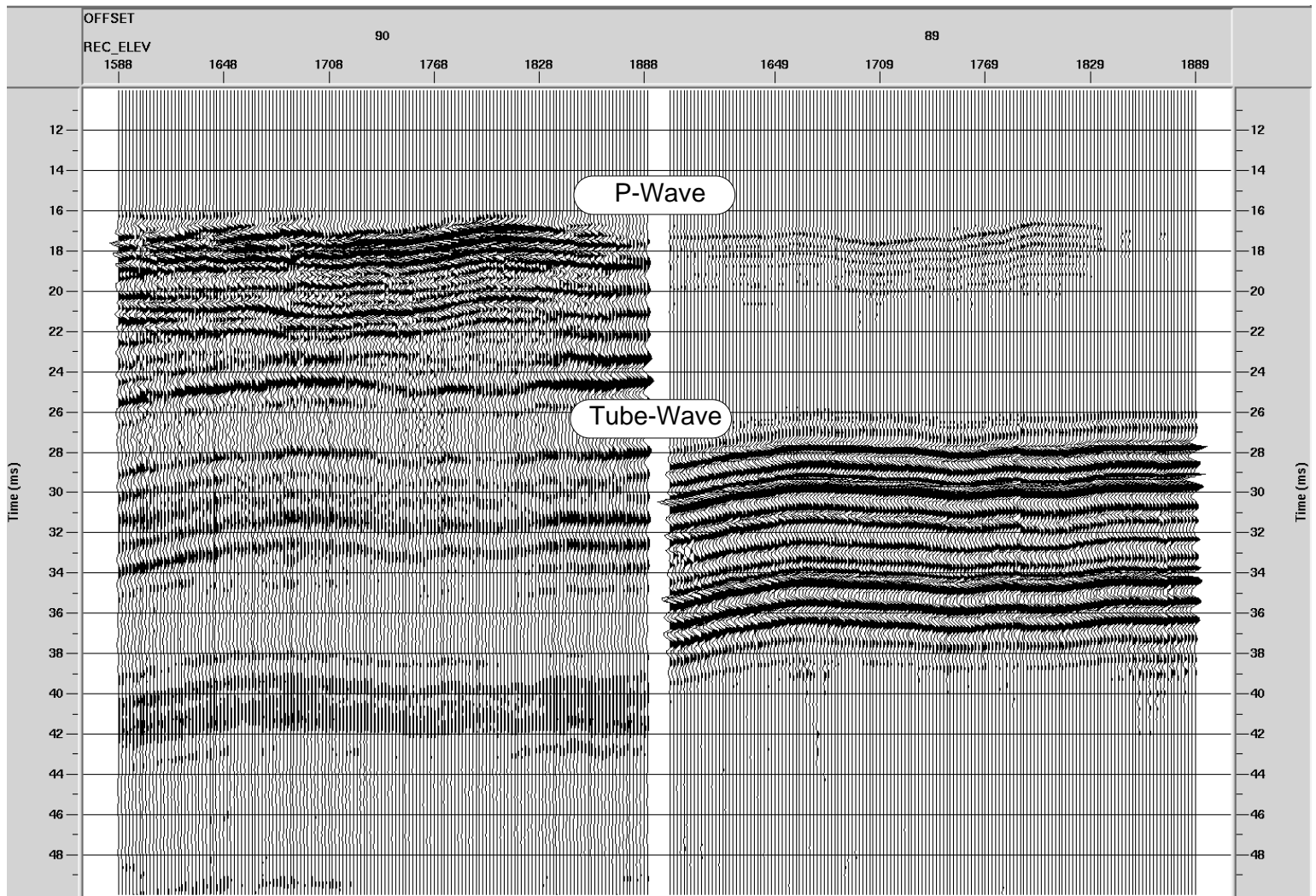


Figure 4. Common offset gathers of single-well seismic data recorded with (left) and without (right) a tube-wave suppressor. Both data sets were acquired with a piezoelectric source and hydrophone receivers. Each trace is normalized by its own maximum amplitude. The reduction in tube-wave energy with respect to the P-wave energy is easily visible.

0 dB <=> Amplitude = 0.441E+01
 RELEV : 1800,1798,1796,1794,1792,1790,1788,1786,
 1784,1782,1780,1778,1776,1774,1772,1770

0 dB <=> Amplitude = 0.418E+04
 RELEV : 1801,1799,1797,1795,1793,1791,1789,1787,
 1785,1783,1781,1779,1777,1775,1773,1771

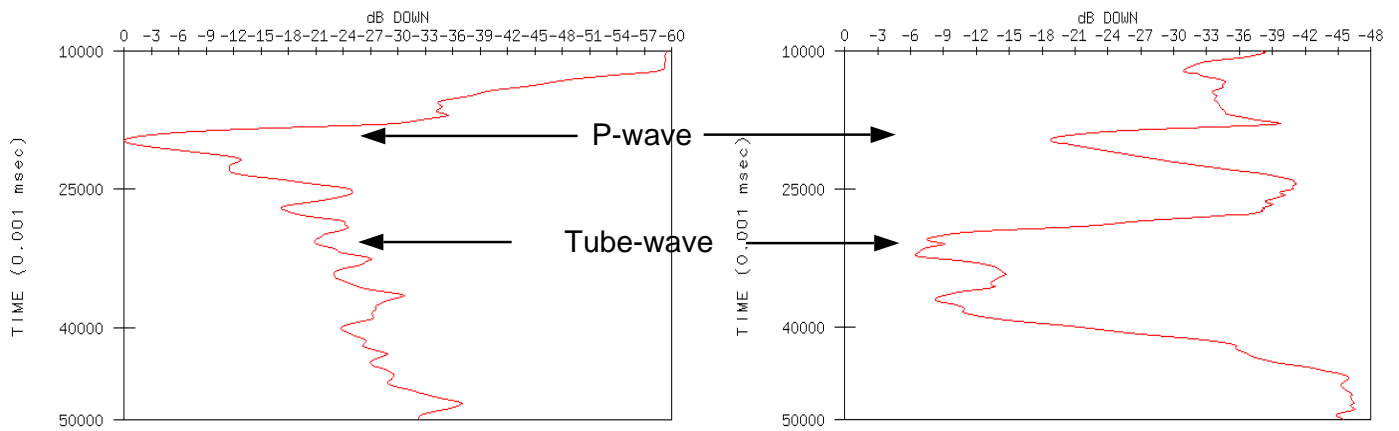


Figure 5 Amplitude analysis of piezoelectric source singlewell data recorded with (left) and without (right) the TWS. The amplitudes are RMS in dB down from the maximum for a moving window averaged over 16 traces. The data without TWS has peak amplitude (0 dB) from source electrical crosstalk at zero time (not plotted). Comparison of the plots shows the TWS has increased the ratio of P-wave to Tube-wave RMS amplitude by 33 dB (21 dB + 12 dB).

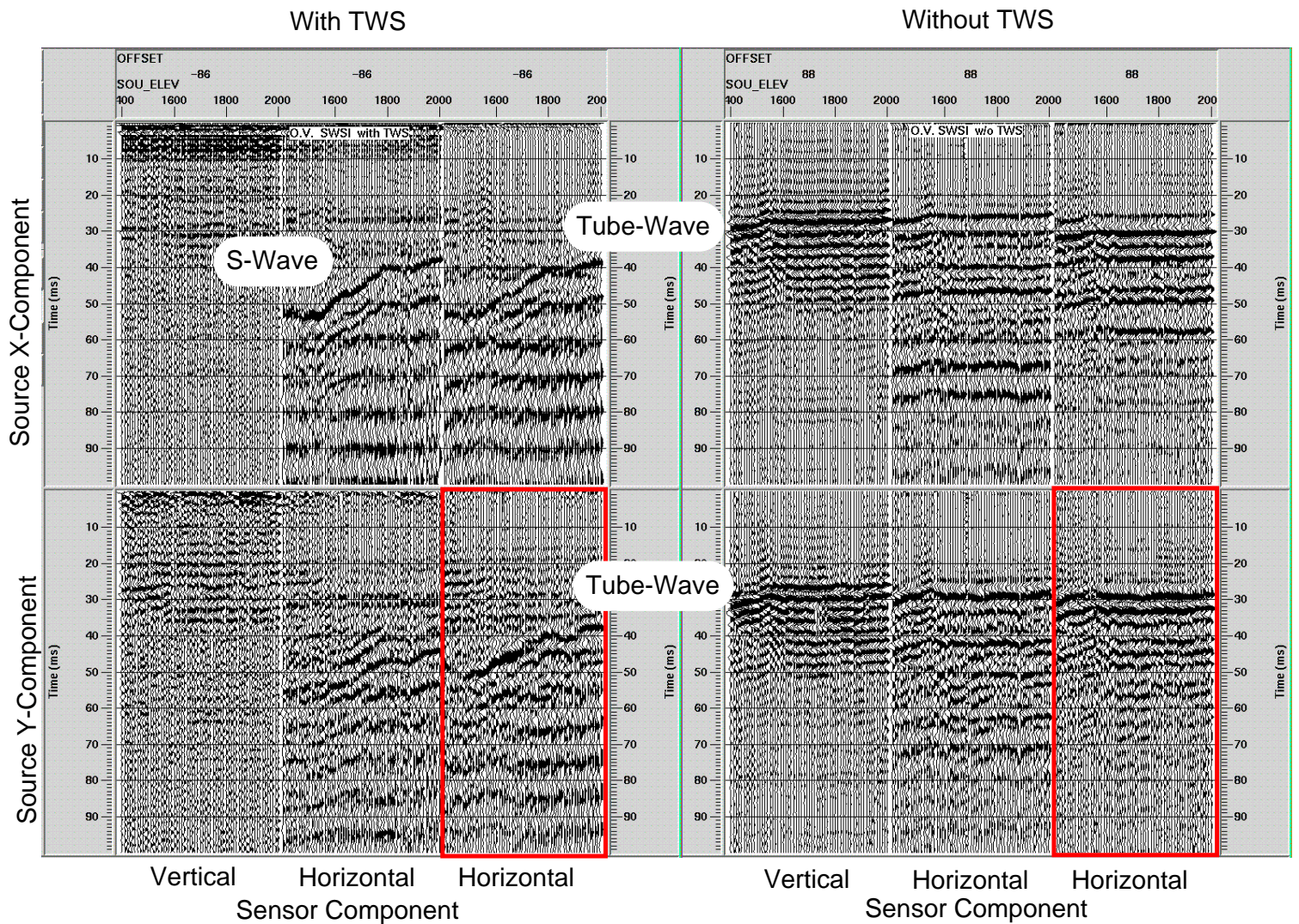


Figure 6 6-component single well data acquired with the orbital vibrator source and 3-component wall-locking geophone sensors. These data are a common offset gather (offset = 86 ft with TWS on left and 88 ft without TWS on right). The top and bottom rows are the two source components (X and Y) as measured by the three sensor components (Z, X, and Y). The data has been trace normalized (each trace normalized to its own maximum). The horizontal component data outlined in red was selected for analysis and is shown in Figure 7.

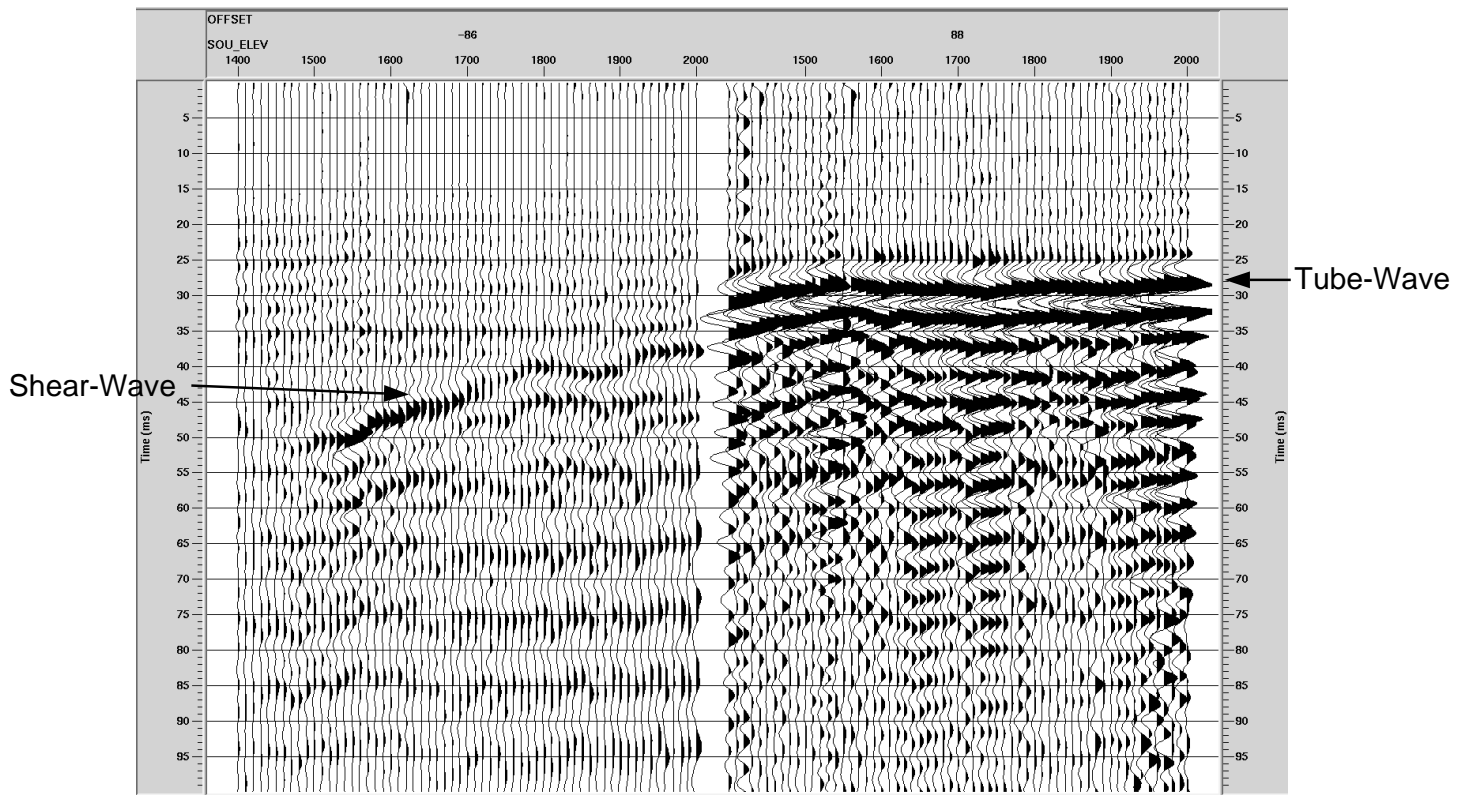


Figure 7. Orbital-vibrator source, single-well data in a common offset gather for a horizontal geophone with TWS (left) and without TWS (right) Data are shown at true relative amplitude. The reduction in tube-wave energy when using the TWS is sufficient to allow identification of a shear-wave arrival (left), which is not identifiable in the data without a TWS (right).

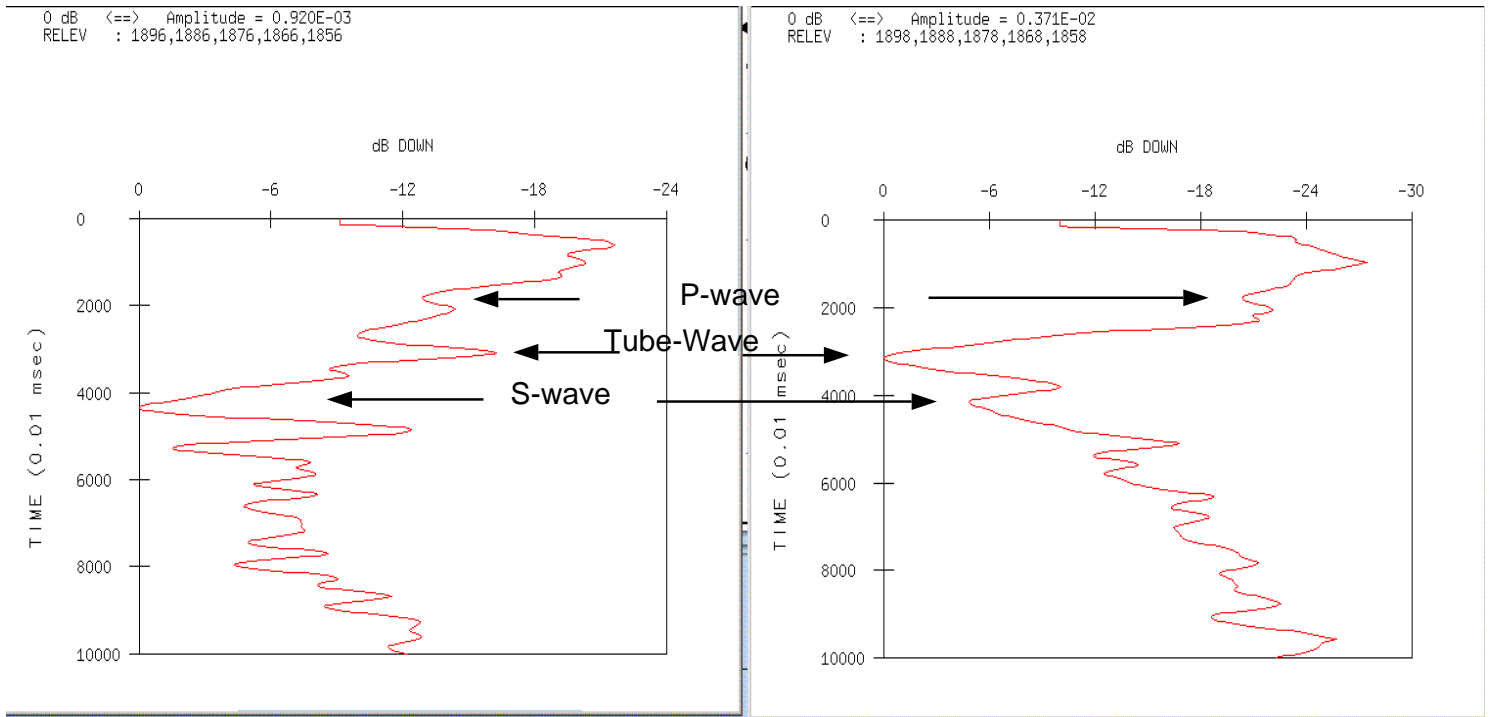


Figure 8 RMS amplitude analysis of orbital vibrator single well data recorded with (left) and without (right) a TWS. For the data recorded without a TWS, the tube-wave is the largest arrival. In data recorded with the TWS, the S-wave is the largest amplitude arrival. Comparing the amplitudes at the S-wave arrival time, we observe a 21 dB improvement in S-wave to tube-wave amplitude ratio. The improvement in P-wave to tube-wave amplitude ratio is 23 dB.